

Published in final edited form as:

J Org Chem. 2013 June 7; 78(11): 5142–5152. doi:10.1021/jo302783d.

Isotope Effects and Mechanism of the Asymmetric BOROX Brønsted Acid Catalyzed Aziridination Reaction

Mathew J. Vetticatt*, Aman A. Desai, and William D. Wulff*

Department of Chemistry, Michigan State University, East Lansing, Michigan 48824

Abstract

The mechanism of the chiral VANOL-BOROX Brønsted acid catalyzed aziridination reaction of imines and ethyldiazoacetate has been studied using a combination of experimental kinetic isotope effects and theoretical calculations. A stepwise mechanism where reversible formation of a diazonium ion intermediate precedes rate-limiting ring-closure to form the *cis*-aziridine is implicated. A revised model for the origin of enantio- and diastereoselectivity is proposed based on relative energies of the ring closing transition structures.

Introduction

The Brønsted acid catalyzed reaction of imines (**1**) and diazo nucleophiles (**2**) can at first glance appear to be a capricious reaction. While reactions of *N*-diarylmethyl or *N*-aryl imines with ethyldiazoacetate typically give *cis*-aziridines (*cis*-**4**) as the major product,^{1,2,3} reactions of *N*-acyl imines give alkylation products (**5**) via C-H bond cleavage.⁴ Changing the nucleophile to a secondary diazoacetamide reverses the diastereoselectivity and *trans*-aziridines can be selectively formed.^{5,6} Enamine formation (**6**) typically accompanies all these reaction modes to a greater or lesser degree. A diazonium ion **3**, resulting from the initial carbon-carbon bond forming event, is assumed to be the common intermediate that partitions into these three pathways as shown in Scheme 1. The intermediacy of **3** has been proposed for aziridine forming reaction of imines and diazo compounds that are mediated by both Lewis and Brønsted acids^{7,8,9,10} and some indirect evidence for the intermediacy of **3** has been presented in certain reactions.¹¹

Over the past decade, we have reported and continued to develop a catalytic asymmetric version of the *cis*-selective aziridination reaction of *N*-diarylmethyl imines and ethyldiazoacetate.¹ A typical example is the reaction of 3,3',5,5'-tetramethyldianisylmethyl (MEDAM) imine **1a** and ethyldiazoacetate **2a** catalyzed by the chiral VANOL-BOROX^{1c} Brønsted acid catalyst (**7**) which proceeds with excellent yield and enantioselectivity, to give almost exclusively one enantiomer of the *cis*-aziridine **4a** with typically a maximum of 1-3% of the enamine side-product **6** (Scheme 2).^{1a} Does this aziridination reaction proceed via a stepwise mechanism (as shown in Scheme 1) or is a concerted mechanism, where all bonds are formed and broken in one transition state, a reasonable possibility?¹² If a diazonium ion intermediate (**3**) is formed (stepwise mechanism), does the subsequent ring-closure step to form the aziridine (**4**) occur via a S_N2-like pathway (where ring-closure and elimination of N₂ occur in one step) or is a S_N1 pathway with formation of a discrete carbocation intermediate possible? The primary focus of this work is to address these fundamental

*mjvcatt@gmail.com, wulff@chemistry.msu.edu.

Supporting Information **Available**. Computational and spectroscopic details and discussions, relevant pdb files, coordinates of all calculated structures. This material is available free of charge at <http://pubs.acs.org>.

questions about the mechanism of the title reaction. We recently published a computational study, where we examined the origin of the *cis*-selectivity observed in this reaction.¹⁰ In doing so, we assumed a stepwise mechanism with the formation of the diazonium ion intermediate as the rate-limiting step. This assumption was a reasonable one, since the entropically favored intramolecular ring closure step that follows diazonium ion formation is expected to be facile. Although this mechanism has been suggested as the most reasonable possibility,^{7b,11} it has not been addressed experimentally in any related aziridination reaction. The >50:1 *cis:trans* ratio was explained on the basis of the lower energy of the transition state for the carbon-carbon bond formation along the *cis*-pathway. This work also aims to provide an experimental basis for the mechanistic assumptions that formed the basis of the transition state model proposed in Ref. 10.

Kinetic isotope effects (KIEs) provide valuable information about the rate-limiting transition state geometry of a reaction. Singleton and coworkers have pioneered the determination of ¹³C KIEs employing NMR methodology at natural abundance.¹³ The experimental isotope effects thus determined can be quantitatively associated to a reaction mechanism by modeling the relevant transition state geometries using computational methods. This approach has been successfully used to probe the mechanism of several fundamental organic reactions.¹⁴ We report here, using this combined experimental and theoretical approach, a detailed insight into the mechanism of the chiral Brønsted acid catalyst (**7**) as it functions in the aziridination reaction of MEDAM imine (**1a**) and ethyldiazoacetate (**2a**).

Results and Discussion

Experimental ¹³C Isotope Effects

The reaction of **1a** and **2a** catalyzed by (*R*)-VANOL-BOROX catalyst **7** was chosen for the determination of intermolecular KIEs by analysis of product.¹⁵ For a bimolecular reaction, this is typically accomplished by comparative NMR analysis of the ¹³C isotopic composition of two product samples, one isolated from a low conversion (~20%) reaction versus one isolated from a reaction taken to 100% conversion, for each of the reactants. This approach requires isolation of four product samples to obtain one complete set of isotope effects for a bimolecular reaction.

A simple modification of this methodology, illustrated in Scheme 2, accomplishes the same goal but with half the effort. Each experiment consists of two reactions. The first reaction was performed using **1a** as the limiting reagent, five times excess of **2a**, and 20 mol % (*R*)-VANOL-BOROX catalyst **7** (with respect to the limiting reagent). The product **4a** isolated from this reaction (labeled “Sample A” in Scheme 3) has undergone partial conversion (20 ± 2 %) in **2a** and quantitative conversion in **1a**. The second reaction was performed under identical conditions, except that the stoichiometry of **1a** and **2a** was reversed. The product **4a** isolated from this reaction (labeled “Sample B” in Scheme 3) has undergone partial conversion (20 ± 2 %) in **1a** and quantitative conversion in **2a**.¹⁶

The ¹³C composition of these samples A and B was compared with each other by NMR analysis. The peak for the methyl carbon of the ester moiety was used as a standard for integration in the NMR analysis with the assumption that the isotope effect at this position is negligible. From the changes in ¹³C isotopic composition and the reaction conversions, the intermolecular ¹³C KIEs were calculated in a standard way.¹⁷ The resulting ¹³C KIEs for the two key bond forming carbon atoms C1 (the iminium carbon of **1a**) and C2 (the nucleophilic carbon of **2a**), obtained from a set of two independent experiments (four total reactions) with six measurements per experiment, are shown in Figure 1.¹⁸

In a catalytic reaction, the KIEs report on bonding changes occurring up to the first irreversible step between free substrate and product. The magnitude of the KIEs is indicative of the extent of bond forming/breaking occurring at the transition state geometry of this irreversible step. The near unity KIE on the iminium carbon (C1) suggests that it does not participate in this isotope sensitive step. This establishes two key aspects of the mechanism, (a) a concerted one-step mechanism is unlikely since such a mechanism would have resulted in a larger KIE on C1 and (b) assuming a stepwise mechanism, the initial carbon-carbon bond forming step to form the diazonium ion intermediate is reversible since irreversible carbon-carbon bond formation would also have resulted in a significant KIE on C1. The large KIE on C2 suggests involvement of this carbon atom in the KIE-determining transition state. Hence the qualitative interpretation of the experimental KIEs is that the aziridination reaction of **1a** and **2a** proceeds via a stepwise mechanism. The carbon-carbon bond-forming step to form the diazonium ion intermediate *precedes* the first irreversible step in the catalytic cycle.¹⁹ A detailed examination of different possible stepwise mechanisms is required for the quantitative interpretation of the experimental KIEs.

Theoretical Analysis of Reaction Mechanism

We have already established, using experiment and theory, the mode of catalysis of this unique chiral BOROX catalyst.^{1b, 1c, 10} The current work builds on the findings in reference 10 and presents a comprehensive analysis of the geometries, energies, and KIEs of all mechanistically relevant transition structures. All transition structures for the (*S*)-VANOL-BOROX catalyzed reaction²⁰ of **1a** and **2a** were located in ONIOM(M062×/6-31+G**:*AM1*) calculations²¹ as implemented in Gaussian 09.²² The division of layers for the ONIOM calculations is shown in Figure 2. All reported distances are in angstroms. Energies of all transition structures/intermediates reported in this work are Gibbs free energies from the ONIOM calculations and are relative to the (catalyst-**1a** complex + **2a**) combination (which is assumed to be 0.0 kcal/mol).

Possible mechanisms based on experimental KIEs

The experimental KIEs (Figure 1) provide persuasive evidence for the reversible formation of a diazonium ion intermediate. Also, the first irreversible step in the catalytic cycle likely follows this diazonium ion formation. In order to correctly interpret our experimental KIEs, we explored three reasonable stepwise mechanisms assuming the initial carbon-carbon bond-forming step to be reversible.

(A) S_N2-like mechanism

This is the widely accepted mechanism for this reaction.^{7,8,9,10,11} However, there is little evidence in the literature with regard to the existence of the diazonium ion intermediate or the identity of rate-limiting step in this mechanism.^{7b,11} Based on our experimental KIEs, we propose that reversible formation of the catalyst bound diazonium ion intermediate (*gauche 3a'*/*anti 3a'*) could be followed by an irreversible S_N2-like ring-closure step (rate-limiting step) to form the aziridine with concomitant elimination of N₂ (Scheme 4). At the transition state for this step, C2 would have bond order to both the intramolecular nucleophile and the leaving group which are in an *antiperiplanar* orientation (*anti 3a'*). This could account for the large observed KIE on C2. In this section, we discuss the results from a comprehensive evaluation of the reaction coordinate for the S_N2-like mechanism **1a**

TS1 is the lowest energy transition structure for the nucleophilic addition of **2a** to the iminium ion of **1a** (Figure 3, A). This transition structure is sustained by multiple non-covalent interactions that lower barrier to catalysis (see expanded view). The protonated imine **1a** is bound to oxygen atom O3 of the boroxinate core of the catalyst via a short, strong hydrogen bond (H-bonding interaction at 2.17 Å). There is also π-stacking between

the phenyl substituent of the imine **1a** and the boroxinate core. A H-bonding interaction between the α -CH of **2a** and oxygen atom O1 (1.94 Å) facilitates the *S_i*-facial attack of **2a**.²³ Electrostatic interactions of the polarized N₂ moiety with the boroxinate oxygen O2 (2.67 Å) and the iminium nitrogen (2.95 Å) further stabilize this transition structure.²⁴

The initial carbon-carbon bond forming step (TS1) results in a catalyst bound *gauche* diazonium ion intermediate (**gauche 3a'**) which maintains all the stabilizing interactions present in TS1 (Figure 3, B). Before S_N2-like nucleophilic attack can occur to close the ring, the activated leaving group (-N₂⁺) should be anti-periplanar to the trajectory of the intramolecular nucleophile. A conformational change occurs, involving rotation of the imine portion of the diazonium ion intermediate while maintaining the H-bonding interaction between the α -CH and O1 (2.05 Å), resulting in **anti 3a'** (Figure 3, C). The dihedral angle defined by the 4 atoms highlighted as spheres in B and C in Figure 3 changes from 24° to -174° on going from **gauche 3a'** to **anti 3a'**. The key difference between B and C (Figure 3) is that the imine-NH...O3 H-bond (2.38 Å) in **gauche 3a'** is replaced by an intramolecular catalyst-independent H-bonding interaction in **anti 3a'** – between the imine -NH and the carbonyl oxygen of the ester moiety (2.32 Å) of the diazonium ion intermediate.

TS2 is the lowest energy transition structure for the S_N2-like ring closure to form **4a** with elimination of N₂ and has a geometry very similar to **anti-3a'** (Figure 4). The H-bonding interaction between the α -CH and O1 remains intact (1.97 Å). The intramolecular H-bond between the imine nitrogen and the carbonyl oxygen of the ester moiety is maintained (2.43 Å), as the C-N bond forms. The diazonium carbon atom C2 has significant bond order to both nucleophile and leaving group, analogous to a classical S_N2 transition state.

Formation of side products

Commonly observed side-products in these reactions are enamines.^{1a,7a,8} These products presumably arise from elimination of the N₂ leaving group from the diazonium ion intermediate **3a** by migration of either the hydrogen atom or the phenyl substituent from C1 to C2 (instead of ring-closure to form *cis*-**4a** as described in Figure 4). This results in an iminium ion intermediate which subsequently is deprotonated to the more stable enamine product as shown in the reaction scheme in Figure 5. Transition structures were located, for the migration of a hydride (**TS2-H-migration**) and the phenyl group (**TS2-phenylmigration**) from C1 to C2. In each of these transition structures, the migrating group is anti-periplanar to the -N₂ leaving group. The product ratio ultimately depends on the relative energies of the three transition structures shown in Figure 5, all of which emanate from the common diazonium ion intermediate **3a**.

The transition structures **TS2-phenylmigration** and **TS2-H-migration** are higher in energy than **TS2** by 3.7 and 7.7 kcal/mol, respectively, consistent with 1-3 % prevalence of these products in the reaction with MEDAM imines.^{1a} The triflic acid catalyzed aziridination reaction of an analogous imine (with a benzhydryl protecting group) and the same diazo nucleophile gives significant amounts of enamine side-products.² We believe that it is the superior stabilization of **TS2** relative to enamine transition structures, by the (*S*)-VANOL-BOROX counterion as compared to the triflate anion, that is responsible for the contrastingly high selectivity observed for the aziridine product in our reaction (proton is the catalyst in both reactions).

(B) S_N1 mechanism

A reasonable alternative is an S_N1 mechanism with dissociation of N₂ from the diazonium ion intermediate as the first irreversible step (Scheme 5). This will lead to the formation of a contact ion pair between the anionic boroxinate catalyst and the resulting carbocation

intermediate. Such a step would be followed by rapid capture of this carbocation by the intramolecular nitrogen nucleophile to give the aziridination product.

Within the framework of such a mechanism, the dissociation of N_2 from the diazonium ion intermediate would be the first irreversible step and the KIEs would reflect the transition state geometry for this step. How the resulting carbocation forms the aziridination product will be of interest only if the S_N1 -transition state geometry is energetically feasible and reproduces the experimental KIEs. We therefore located a transition structure, TS2- S_N1 , for the irreversible formation of the catalyst bound carbocation from **gauche 3a'** (Figure 6). This was a challenging task since as the N_2 moiety dissociates from **gauche 3a'**, there is a propensity for the groups on C1 to migrate to the carbocationic center (C2) resulting in an iminium ion intermediate which eventually forms the enamine side product (as described in Figure 5). TS2- S_N1 has a geometry that is characterized by the same interactions that stabilize **gauche 3a'**, the only difference being the elongated C2-leaving group ($-N_2^+$) bond (2.2 Å). This leads to significant carbocation character on C2, characteristic of S_N1 transition states.

(C) Miscellaneous mechanisms

There are two additional possibilities that can be imagined that would seem consistent with the experimental KIEs. One of these involves nucleophilic participation of the boroxinate anion to displace N_2 from the diazonium ion intermediate resulting in a covalently bound catalyst-substrate complex.²⁵ The aziridine **4a** can then be formed by a 'double displacement' mechanism with regeneration of the catalyst as shown in Scheme 6 A. Alternatively the experimental KIEs could also result from a late asynchronous concerted transition structure where all bond-making and bond-breaking occur in one chemical step (Scheme 6 B). Despite our best efforts and rigorous exploration of the reaction surface, saddle points could not be located for either of these possibilities.

Energetic considerations and predicted KIEs for calculated mechanisms

The stationary points along the reaction coordinate for the S_N1 and S_N2 -like mechanisms are shown in Figure 7 along with their free energy estimates relative to the catalyst-**1a** complex and **2a**. The KIEs for all transition structures in Figure 7 were predicted from their scaled theoretical vibrational frequencies based on conventional transition state theory using the program ISOEFF 98.²⁶ Tunneling corrections were applied to the predicted KIEs using a one-dimensional infinite parabolic barrier model.²⁷ The reaction coordinate shown in black represents the S_N2 -like mechanism. The key result of note here is that the rate-limiting step (highest free energy barrier) in this mechanism is the intramolecular S_N2 -like ring closure to form *cis*-**4a** (TS2). All preceding transition structures (TS1 and TS_{rot}), result in high energy intermediates (**gauche 3a'** and **anti 3a'**, respectively) that face a higher barrier to go forward than reverse along the reaction coordinate. The KIEs should therefore reflect the geometry of TS2, the first irreversible step between free starting material and product along the reaction coordinate.

The reaction coordinate for the S_N1 pathway is identical to the S_N2 -like mechanism up until formation of **gauche 3a'**. TS2- S_N1 , the transition structure for the dissociation of N_2 from **gauche 3a'**, is the rate-limiting step in the S_N1 pathway. TS2- S_N1 is 10.2 kcal/mol higher in energy than the rate-limiting step in the S_N2 -like pathway. Based on energetics alone, the S_N2 -like mechanism appears to be more likely than the S_N1 mechanism. Further support for the S_N2 -like mechanism is obtained from the theoretical prediction of KIEs of the relevant transition structures. The predicted KIEs for carbon atoms C1 and C2, assuming each of the transition structures TS1, TS_{rot}, TS2, and TS2- S_N1 to be KIE determining, are shown in Figure 7 along with the experimental KIEs. The predicted KIEs for TS2 are in excellent

agreement with the experimental KIEs for both C1 and C2. Additionally, the predicted KIEs for TS1, TS_{rot}, and TS2-S_N1 are clearly inconsistent with the experimental values. The energy considerations and the quantitative match of experimental and predicted KIEs for TS2, taken together, provides strong support for a stepwise mechanism with reversible formation of a diazonium ion intermediate followed by rate-limiting S_N2-like ring closure to form *cis*-**4a**.

Re-evaluation of the origin of *cis*-diastereoselection and enantioselectivity

In our earlier study, we rationalized the *cis*-selectivity observed in the (*R*)-VANOL-BOROX catalyzed aziridination reaction of **1a** and **2a** based on the relative energy of the carbon-carbon bond forming (eg. TS1) transition structures along the diastereomeric pathways leading to *cis*- and *trans*-aziridines (*cis* favored over *trans* by 3.1 kcal/mol based on B3LYP/6-31+G* single point energies performed on ONIOM(B3LYP/6-31G*:AM1) optimized transition structures).¹⁰ In addition to assuming a stepwise mechanism, we had also made the reasonable assumption that the entropically disfavored nucleophilic addition of **2a** to **1a** was the rate-limiting step of the reaction.¹² While our assumption about the stepwise mechanism was correct, the experimental KIEs reported in this work clearly establishes that it is the intramolecular S_N2-like ring closure and not the addition step that is rate-limiting. Our explanation of the origin of the observed *cis*-diastereoselection thus warrants a re-evaluation. Having experimentally established the rate-limiting step in the *cis*-pathway and validated it by calculations, we decided to carry out a calculational analysis of the reaction coordinate for the formation of *trans*-**4a**.²⁸ A comparison of the relative energies of the rate-limiting steps along each pathway would then constitute our revised model for the origin of *cis*-diastereoselection observed in this reaction.

It has been established that *trans*-**4a** (minor diastereomer) formed in this reaction has the opposite facial selectivity to the imine as compared to *cis*-**4a**.²⁹ We therefore modeled the attack of **2a** on the *re*-face of **1a** (as opposed to the *si*-facial attack in TS1). Structure TS3 (Figure 8, A) is the lowest energy carbon-carbon bond forming transition structure leading to the diazonium ion intermediate along the *trans*-pathway. Comparison of the expanded view of TS3 in Figure 8 to that of TS1 in Figure 3 reveals a very similar geometry of the catalyst and **2a**. The only difference between TS3 and TS1 is the face of catalyst bound-**1a** that is exposed to attack by **2a**. As a result, the diazonium ion formed from TS3 (**trans anti 3a'**) has an anti-periplanar orientation of the N(imine)-C1-C2-N(diazo) bond (highlighted as spheres in Figure 8 B) and is already “set up” for S_N2-like ring closure, without an intervening bond rotation event as in the *cis*-pathway (See Figure 7, TS_{rot}). Figure 8 C shows the transition structure for the formation of *trans*-**4a**. It is important to note that unlike the *cis*-pathway, all transition structures and intermediates in the *trans*-pathway are stabilized by the same non-covalent interactions, namely (a) the imine NH—O3 hydrogen bond, (b) the α-CH—O1/O2 hydrogen bond and (c) the electrostatic interaction between the polarized N₂ leaving group and O1. As a result, the addition and ring closing transition structures in the *trans*-pathway (TS3 and TS4) are much closer in energy than their counterparts in the *cis*-pathway.

A comparison of the free energy profiles for the reaction coordinates of the diastereomeric aziridination pathways is shown in Figure 9. The transition structure for the S_N2-like ring closure is the highest barrier (rate-limiting step) along both diastereomeric pathways, though the difference between TS3 and TS4 (0.6 kcal/mol) is not as significant as the difference between TS1 and TS2 (4.0 kcal/mol). Comparison of the relative energies of TS2 and TS4 gives a theoretical *cis:trans* ratio of ~10:1. This is in reasonable agreement with the experimental >50:1 *cis:trans* ratio observed for this reaction. Therefore based on the experimental KIEs and calculations presented in this work we wish to revise our hypothesis

on the origin of *cis* diastereoselection observed in the title reaction. We propose that the observed diastereoselectivity is a result of the lower energy of TS2 as compared to TS4, the rate-limiting steps in each of the diastereomeric pathways. Finally, calculations accurately predict the enantioselectivity of the reaction – TS1-*ent*, the carbon-carbon bond forming transition structure for the minor enantiomer of *cis*-**4a** was found to be 3.9 kcal/mol higher in energy than TS1 while TS2-*ent*, the ring-closing transition structure for the minor enantiomer of *cis*-**4a** was also found to be 3.9 kcal/mol higher in energy than TS2 – consistent with the experimentally observed 99 % ee.³⁰ Therefore Figure 9 provides a new basis for the observed enantio- and diastereoselectivity of the reaction – the relative energies of the respective ring-closing transition structures.

Conclusion

Experimental KIEs unambiguously reveal the mechanism of the (*R*)-VANOL-BOROX catalyzed aziridination reaction of MEDAM imine **1a** and ethyl diazoacetate. The near unity ¹³C KIE for the iminium carbon atom of **1a** and the large ¹³C KIE of ~ 5% on the α -carbon of ethyl diazoacetate suggests that the first irreversible step in the catalytic cycle is the ring-closure to form the *cis*-aziridine. This is the first experimental study that provides direct evidence for a stepwise mechanism involving the formation of a diazonium ion intermediate. The predicted KIEs, for S_N2-like intramolecular ring-closure to form the *cis*-aziridine from the diazonium ion intermediate, are in quantitative agreement with the experimental KIEs. Detailed theoretical analysis of the reaction energy profile reveals reversible formation of the diazonium ion intermediate followed by rate-limiting ring-closure, consistent with interpretation of the observed KIEs.

The identification of the rate-limiting step led to a re-evaluation of the origin of enantio- and diastereoselectivity observed in this reaction. Calculations suggest that the rate-limiting step, in both the diastereomeric pathway leading to *trans*-aziridine and the enantiomeric pathway leading to the minor enantiomer of *cis*-**4a**, is the intramolecular ring-closure. The > 50:1 *cis:trans* ratio and 99 % ee observed in this reaction is now explained on the basis of the relative energies of the competing S_N2-like ring-closing transition structures. We are currently exploring the generality of this reaction mechanism for other Lewis/Brønsted acid catalyzed aziridination reactions, which are proposed to proceed via similar addition-cyclization-elimination pathways. The results from these studies will be reported in due course.

Experimental Section

General

All experiments were performed under an Argon atmosphere. Flasks were flame dried and cooled under Argon before use. Toluene was dried from sodium under nitrogen. The VANOL ligand is commercially available from Aldrich as well as Strem Chemicals, Inc. If desired, it could be purified using column chromatography on regular silica gel using an eluent mixture of 2:1 dichloromethane:hexanes. Triphenylborate and ethyldiazoacetate were used as purchased from Aldrich. The preparation of imine **1a** can be found in a previous report from our group.³¹

The silica gel for column chromatography was standard grade, 60 Å porosity, 230 × 400 mesh particle size, 500 – 600 m²/g surface area and 0.4 g/mL bulk density. The ¹H and ¹³C NMR spectra were recorded in CDCl₃, wherein CHCl₃ was used as the internal standard for both ¹H NMR (δ = 7.24) and ¹³C NMR (δ = 77). Analytical thin-layer chromatography (TLC) was performed on silica gel plates with F-254 indicator. Visualization was by short

wave (254 nm) and long wave (365 nm) ultraviolet light, or by staining with phosphomolybdic acid reagent (20% wt in ethanol).

Procedure for the aziridination reactions

Preparation of the catalyst stock solution—A 100 mL glass Schlenk flask fitted with a magnetic stir bar was connected via vacuum tubing to a double manifold vacuum line equipped with an Argon ballast. The Schlenk flask was made in a glass blowing shop by fusing together a high vacuum teflon valve and a 100 mL recovery flask. The side-arm of the high vacuum valve was modified with a piece of 3/8th inch glass tubing to fit with the vacuum tubing attached to the double manifold. The double manifold had two-way high-vacuum valves, which could be alternated between high vacuum (0.1 mm Hg) and an Argon supply (ultra high purity, 99.999%). The Schlenk flask was then flame dried under high vacuum and cooled under a low flow of Argon. To the flask was added sequentially (*R*)-VANOL (463 mg, 1.06 mmol), triphenylborate (1.23 g, 4.23 mmol), dry toluene (20 mL), and water (19 μ L, 1.06 mmol) under a low flow of Argon. The threaded Teflon valve on the Schlenk flask was then closed, and the mixture heated at 80 °C for 1 h. The valve was opened to gradually apply high vacuum (0.1 mm Hg) and the solvent was removed. The vacuum was maintained for a period of 30 min at 80 °C. The flask was then removed from the oil bath and allowed to cool to room temperature under a low flow of Argon. The residue was then completely dissolved in 50 mL of dry toluene to afford the stock solution of the catalyst.

The aziridination reaction – illustrated for Reaction 1 (1st run, Scheme 7)—A 50 mL round-bottom single-neck (24/40 joint) flask fitted with a magnetic stir bar was flame dried under high vacuum and cooled under a low flow of Argon. To the flask was then added imine **1a** (2.05 g, 5.29 mmol, 1 equiv). The flask was then fitted with a rubber septum and an Argon balloon. To this flask was added 10 mL of the catalyst stock solution (20 mol % catalyst with respect to **2**, 0.21 mmol) via a plastic syringe fitted with a metallic needle. To the stirred solution of this catalyst-imine complex was then added ethyldiazoacetate **2** (1.06 mmol, 0.2 equiv). Commercial ethyldiazoacetate from Aldrich usually contains dichloromethane. The exact amount of ethyldiazoacetate was added to the reaction after considering the ratios of ethyldiazoacetate and dichloromethane from ¹H NMR analysis of the commercial ethyldiazoacetate. The reaction mixture was then stirred at room temperature for 15 h.

Work-up, purification, and analysis—The reaction mixture was diluted with hexanes and subjected to rotary evaporation until the solvent was removed. The ¹H NMR analysis of the crude product revealed a conversion of 20%, determined by the relative integration of the aziridine ring methine protons vs. the iminium methine proton. Purification of aziridine **4a** was done via column chromatography with regular silica gel and an eluent mixture of 1:20:20 EtOAc:hexanes:dichloromethane and then 1:10:10 EtOAc:hexanes:dichloromethane. If ¹H NMR analysis of the product after chromatography showed the presence of a phenolic impurity, the product was dissolved in EtOAc and washed twice with 10% aq. NaOH, water, brine, and subsequently dried over Na₂SO₄. This procedure afforded the pure product **4a** as an off-white solid in 95% isolated yield (475 mg, 1.00 mmol). The optical purity of **4a** was determined to be 99% ee by chiral HPLC analysis. Complete characterization details for **4a** can be found in a previous report from our group.³¹ Spectral data for **4a**: ¹H NMR (CDCl₃, 500 MHz) δ 0.99 (t, 3H, *J* = 7.1 Hz), 2.21 (s, 6H), 2.27 (s, 6H), 2.59 (d, 1H, *J* = 6.9 Hz), 3.14 (d, 1H, *J* = 6.9 Hz), 3.63 (s, 3H), 3.69 (s, 3H), 3.69 (s, 1H), 3.93-3.96 (m, 2H), 7.13 (s, 2H), 7.18-7.27 (m, 5H), 7.39 (d, 2H, *J* = 6.9 Hz); ¹³C NMR (CDCl₃, 125 MHz) δ 10.0, 12.2, 12.2, 42.5, 44.3, 55.3, 55.4, 56.4, 73.0, 123.3, 123.6, 123.7, 123.9, 126.5, 126.6, 131.5, 134.0, 134.2, 152.2, 152.3, 163.8.

Supplementary Material

Refer to Web version on PubMed Central for supplementary material.

Acknowledgments

This work was supported by the National Institute of General Medical Sciences (GM 094478).

References

- (1). (a) Mukherjee M, Gupta AK, Lu Z, Zhang Y, Wulff WD. *J. Org. Chem.* 2010; 75:5643–5660. [PubMed: 20704436] (b) Hu G, Gupta AK, Huang RH, Mukherjee M, Wulff WD. *J. Am. Chem. Soc.* 2010; 132:14669–14675. [PubMed: 20863108] (c) Gupta AK, Mukherjee M, Hu G, Wulff WD. *J. Org. Chem.* 2012; 77:7932–7944. [PubMed: 22947019]
- (2). Williams AL, Johnston JN. *J. Am. Chem. Soc.* 2004; 126:1612–1613. [PubMed: 14871074]
- (3). Akiyama T, Suzuki T, Mori K. *Org. Lett.* 2009; 11:2445–2447. [PubMed: 19397337]
- (4). (a) Uraguchi D, Sorimachi K, Terada M. *J. Am. Chem. Soc.* 2005; 127:9360–9361. [PubMed: 15984850] (b) Hashimoto T, Maruoka K. *J. Am. Chem. Soc.* 2007; 129:10054–10055. [PubMed: 17655298]
- (5). Hashimoto T, Uchiyama N, Maruoka K. *J. Am. Chem. Soc.* 2008; 130:14380–14381. [PubMed: 18847267]
- (6). Desai AA, Wulff WD. *J. Am. Chem. Soc.* 2010; 132:13100–13103. [PubMed: 20806892]
- (7). (a) Casarrubios L, Pérez JA, Brookhart M, Templeton JL. *J. Org. Chem.* 1996; 61:8358–8359. (b) Rasmussen KG, Jørgensen KA. *J. Chem. Soc., Perkin Trans 1.* 1997:1287–1292.
- (8). Zhang Y, Lu Z, Wulff WD. *Syn. Lett.* 2009; 17:2715–2739.
- (9). Johnston JN, Muchalski H, Troyer TL. *Angew. Chem. Int. Ed.* 2010; 49:2290–2298.
- (10). Vetticatt MJ, Desai AA, Wulff WD. *J. Am. Chem. Soc.* 2010; 132:13104–13107. [PubMed: 20806891]
- (11). Troyer TL, Muchalski H, Hong KB, Johnston JN. *Org. Lett.* 2011; 13:1790–1792. [PubMed: 21366339]
- (12). By a concerted mechanism we are suggesting that formation of the two bonds between **1** and **2** and loss of N₂ to yield the product aziridinium ion might occur in one step. The preceding protonation of imine and subsequent deprotonation of the aziridinium ion to yield aziridine are distinct mechanistic events.
- (13). Singleton DA, Thomas AA. *J. Am. Chem. Soc.* 1995; 117:9357–9358.
- (14). (a) Beno BR, Houk KN, Singleton DA. *J. Am. Chem. Soc.* 1996; 118:9984–9985. (b) Singleton DA, Merrigan SR, Liu J, Houk KN. *J. Am. Chem. Soc.* 1997; 119:3385–3386. (c) DelMonte AJ, Haller J, Houk KN, Sharpless KB, Singleton DA, Strassner T, Thomas AA. *J. Am. Chem. Soc.* 1997; 119:9907–9908. (d) Keating AE, Merrigan SR, Singleton DA, Houk KN. *J. Am. Chem. Soc.* 1999; 121:3933–3938. (e) Frantz DE, Singleton DA. *J. Am. Chem. Soc.* 2000; 122:3288–3295. (f) Zhu H, Clemente FR, Houk KN, Meyer MP. *J. Am. Chem. Soc.* 2009; 131:1632–1633. [PubMed: 19191687]
- (15). (a) Frantz DE, Singleton DA, Snyder JP. *J. Am. Chem. Soc.* 1997; 119:3383–3384. (b) Singleton DA, Schulmeier BE. *J. Am. Chem. Soc.* 1999; 121:9313–9317.
- (16). See Vetticatt MJ, Singleton DA. *Org. Lett.* 2012; 14:2370–2373. [PubMed: 22506639] for the first report of this modified procedure to measure KIEs by analysis of product. The yields, diastereoselectivity and enantioselectivity of aziridine **4a** obtained under these modified conditions are essentially identical to those obtained using the optimized reaction stoichiometry of 1:1.1 (**1a**:**2a**).^{1a}
- (17). See Supporting Information for method used for calculation of KIEs from the numerical integrations.
- (18). See Supporting Information for KIEs of other carbon atoms and representative NMR spectra.
- (19). Johnston and coworkers (reference 11) have published indirect evidence that the first step involving addition of the diazo compound to the imine is non-reversible under Brønsted acid

catalysis with triflic acid. However, this reaction involves an activated imine derived from methyl glyoxylate and thus there may very well be a mechanism change for this reaction.

- (20). The KIE experiments were performed using (*R*)-VANOL while all calculations were performed using (*S*)-VANOL.
- (21). (a) Svensson M, Humbel S, Morokuma K. *J. Chem. Phys.* 1996; 105:3654–3661.(b) Vreven T, Morokuma K. *J. Comput. Chem.* 2000; 21:1419–1432.(c) Dapprich S, Komáromi I, Byun KS, Morokuma K, Frisch MJ. *J. Mol. Struct.* 1999; 461:1–21.
- (22). Frisch, MJ.; Trucks, GW.; Schlegel, HB.; Scuseria, GE.; Robb, MA.; Cheeseman, JR.; Scalmani, G.; Barone, V.; Mennucci, B.; Petersson, GA.; Nakatsuji, H.; Caricato, M.; Li, X.; Hratchian, HP.; Izmaylov, AF.; Bloino, J.; Zheng, G.; Sonnenberg, JL.; Hada, M.; Ehara, M.; Toyota, K.; Fukuda, R.; Hasegawa, J.; Ishida, M.; Nakajima, T.; Honda, Y.; Kitao, O.; Nakai, H.; Vreven, T.; Montgomery, JA., Jr.; Peralta, JE.; Ogliaro, F.; Bearpark, M.; Heyd, JJ.; Brothers, E.; Kudin, KN.; Staroverov, VN.; Kobayashi, R.; Normand, J.; Raghavachari, K.; Rendell, A.; Burant, JC.; Iyengar, SS.; Tomasi, J.; Cossi, M.; Rega, N.; Millam, NJ.; Klene, M.; Knox, JE.; Cross, JB.; Bakken, V.; Adamo, C.; Jaramillo, J.; Gomperts, R.; Stratmann, RE.; Yazyev, O.; Austin, AJ.; Cammi, R.; Pomelli, C.; Ochterski, JW.; Martin, RL.; Morokuma, K.; Zakrzewski, VG.; Voth, GA.; Salvador, P.; Dannenberg, JJ.; Dapprich, S.; Daniels, AD.; Farkas, Ö.; Foresman, JB.; Ortiz, JV.; Cioslowski, J.; Fox, DJ. *Gaussian 09*. Gaussian, Inc.; Wallingford CT: 2009. Revision **A.1**
- (23). See Figure 2 for the numbering scheme for the boroxinate oxygen atoms.
- (24). Several other higher energy possibilities that lead to the same facial selectivity have been evaluated and are given in the Supporting Information as TS1a-d.
- (25). A similar mechanism was proposed for a reaction catalyzed by dithiophosphoric acids. Shapiro ND, Rauniyar V, Hamilton GL, Wu J, Toste FD. *Nature*. 2011; 470:245–250. [PubMed: 21307938]
- (26). Scott AP, Radom L. *J. Phys. Chem.* 1996; 100:16502–16513. Anisimov V, Paneth P. *J. Math. Chem.* 1999; 26:75–86. The KIE predictions were made by comparison of the vibrational frequencies of the relevant transition structures to that of the lowest energy conformation of the starting material. The predictions are not only for the forward direction for the reversible steps rather they incorporate the equilibrium isotope effects for all reversible steps preceding the transition structure in question.
- (27). Bell, RP. *The Tunnel Effect in Chemistry*. Chapman & Hall; London: 1980. p. 60-63.
- (28). There is no good experimental method to determine the rate-limiting step in the *trans*-pathway since it is formed as a <1:50 minor product in this reaction. Since the energetics of the reaction coordinate for the *cis* pathway was consistent with the interpretation of the experimental KIEs, we believe that we can compare the relative energetics of the *cis* and *trans* pathways using the same calculations.
- (29). See Ref. 6 for a discussion on the facial bias in the formation of the different diastereomers.
- (30). The coordinates and pdb files of the calculated structures TS1-*ent* and TS2-*ent* are available in the Supporting Information.
- (31). Zhang Y, Lu Z, Desai A, Wulff WD. *Org. Lett.* 2008; 10:5429–5432. [PubMed: 18989967]

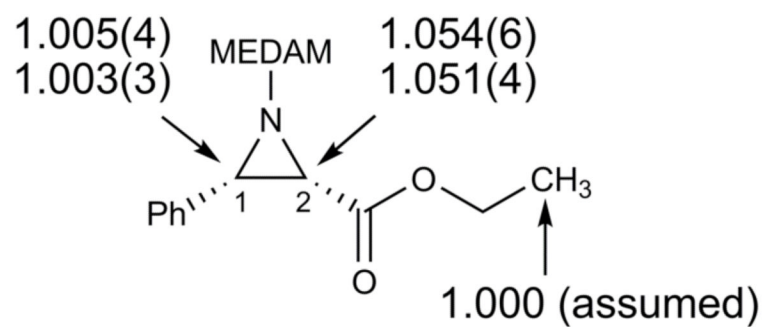


Figure 1. Experimental ^{13}C KIEs ($k_{12\text{C}}/k_{13\text{C}}$) for the aziridination reaction of **1a** and **2a** catalyzed by **7** from two independent experiments with six measurements per experiment. The numbers in parenthesis represent the standard deviation on the last digit from the six measurements of each of the experiments.

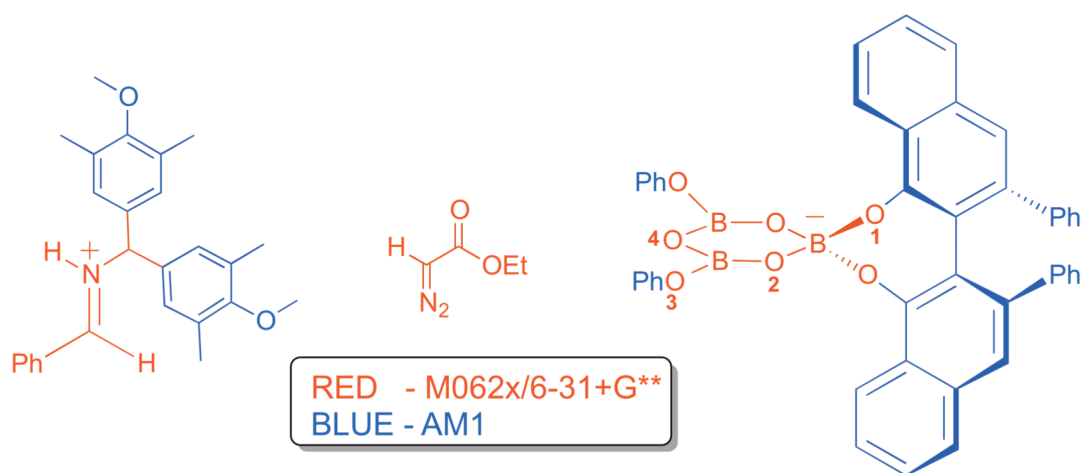


Figure 2. Division of layers for the ONIOM calculations. The portions in red are modeled using the DFT method. The blue portions are calculated using the semi-empirical method.

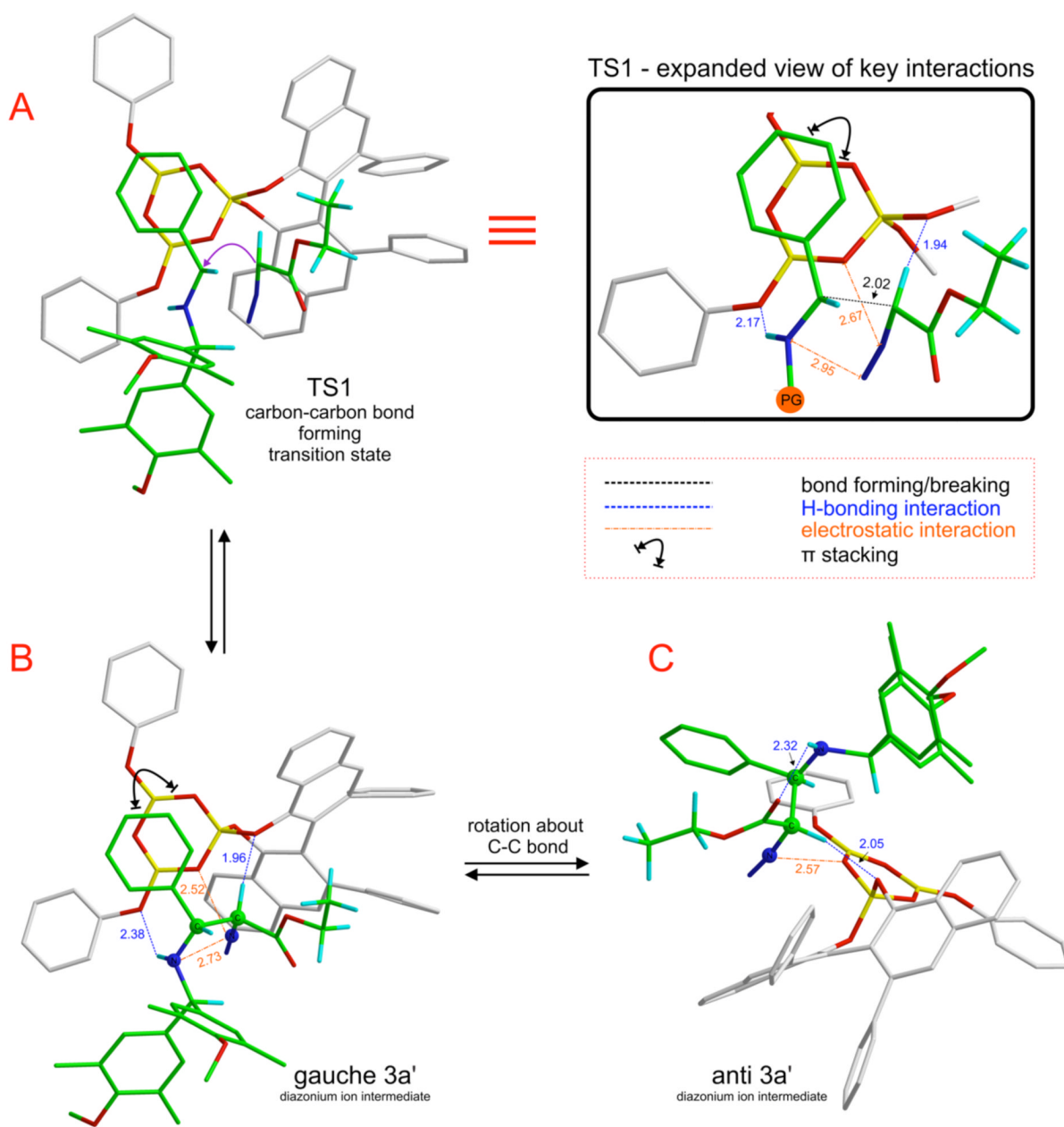


Figure 3.
Reversible steps preceding ring-closure to form *cis*-**4a** in the S_N2 -like mechanism.

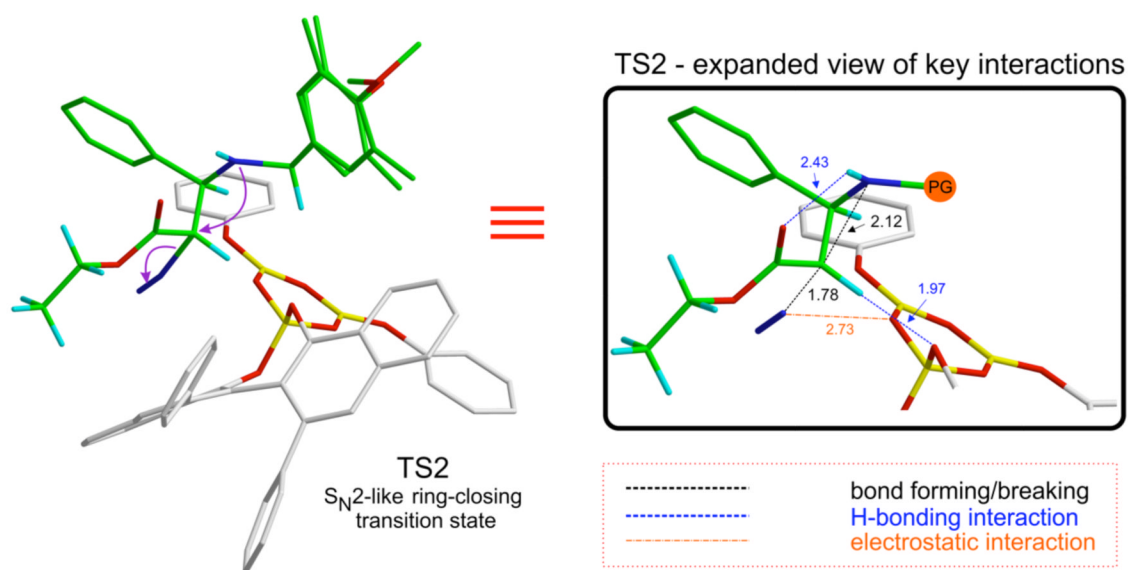


Figure 4. Lowest energy ring-closing transition structure (TS2) giving *cis*-**4a** via the S_N2-like mechanism.

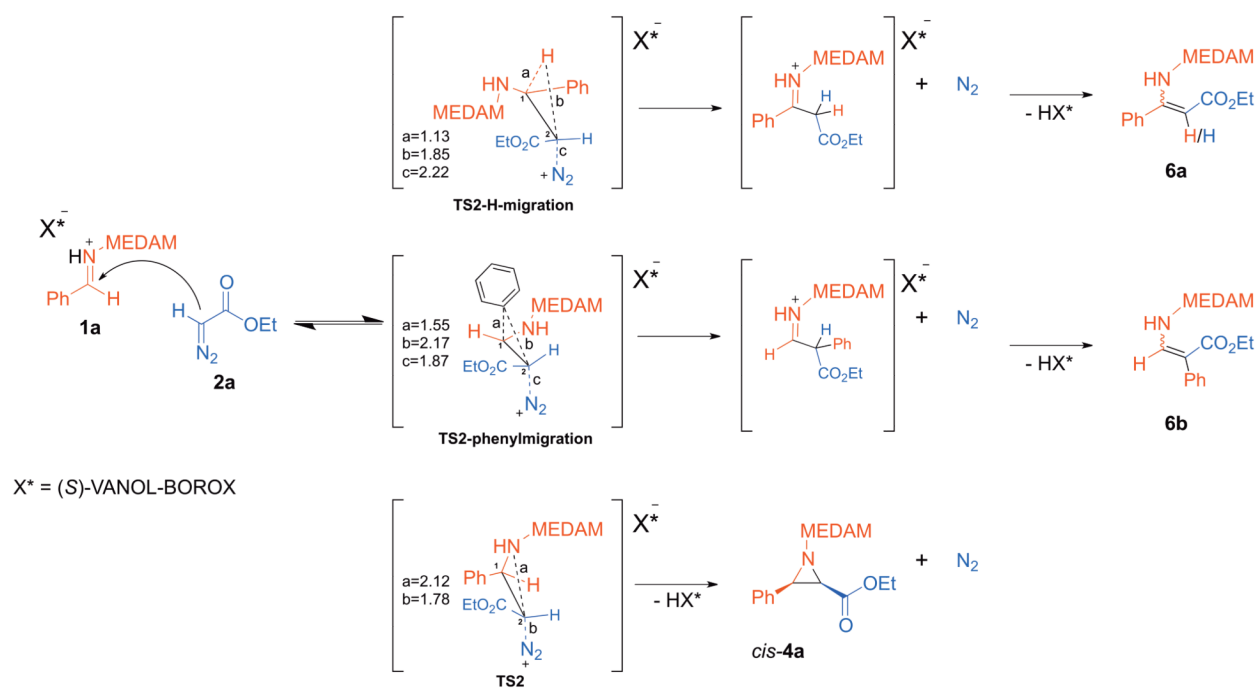


Figure 5. Reaction scheme and transition structures for the formation of enamine side-products **6a/6b** from the common diazonium ion intermediate **3a**. All distances are in Å. TS2 is also depicted for comparison.

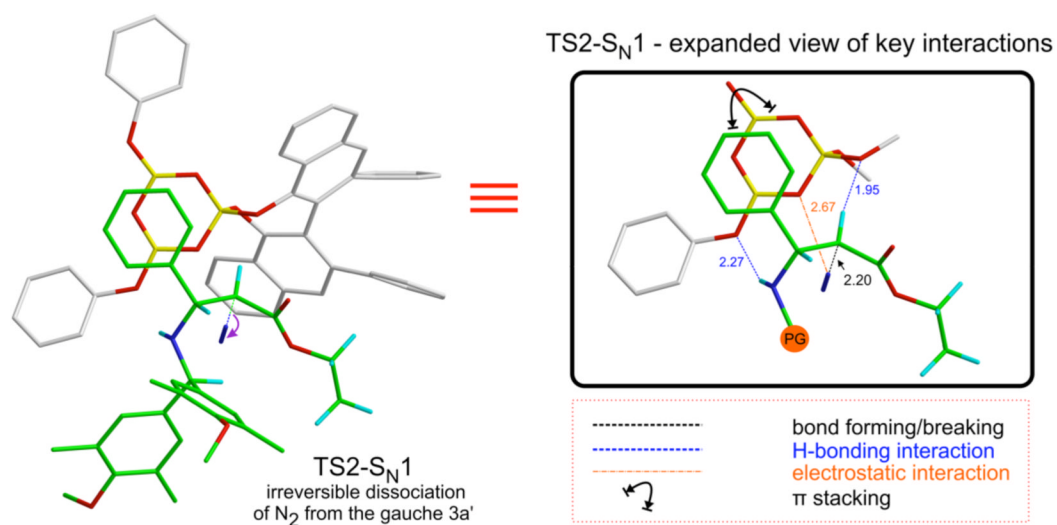


Figure 6. Transition structure (TS2-S_N1) for the irreversible dissociation of N₂ from the diazonium ion.

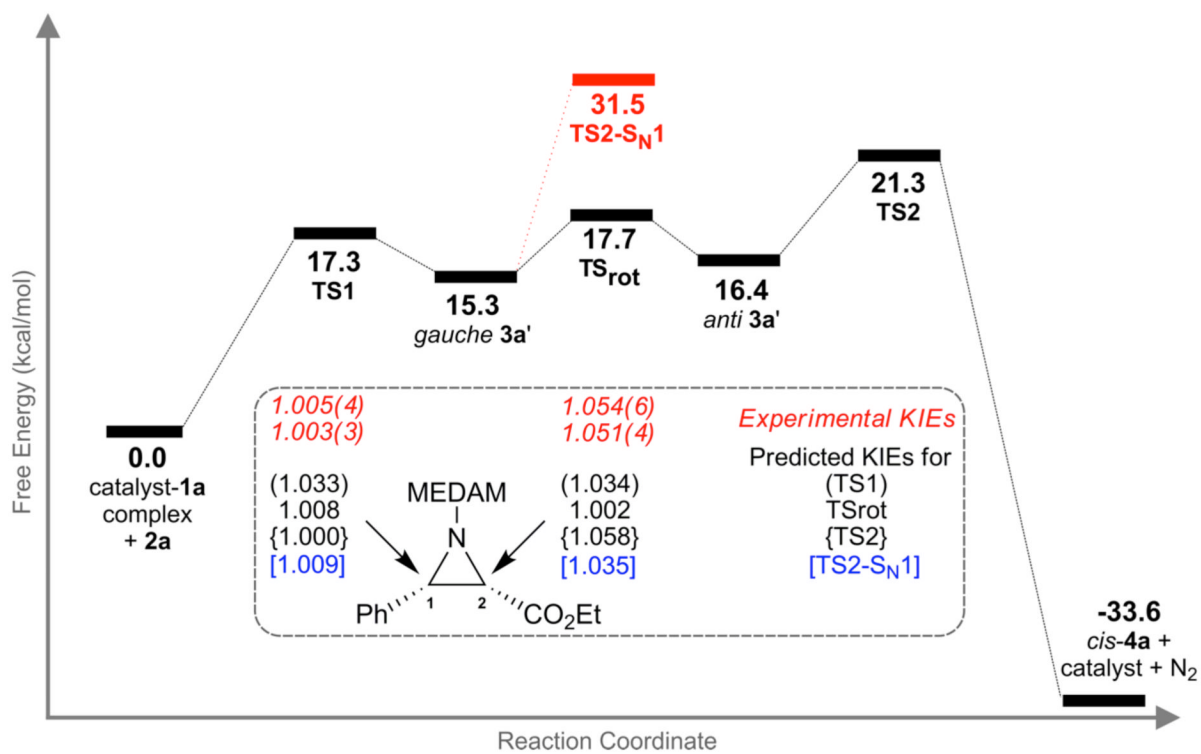


Figure 7. Gibbs free energies (25 °C) for all stationary points along the reaction coordinate along with the predicted KIEs for the S_N2-like and S_N1 mechanisms.

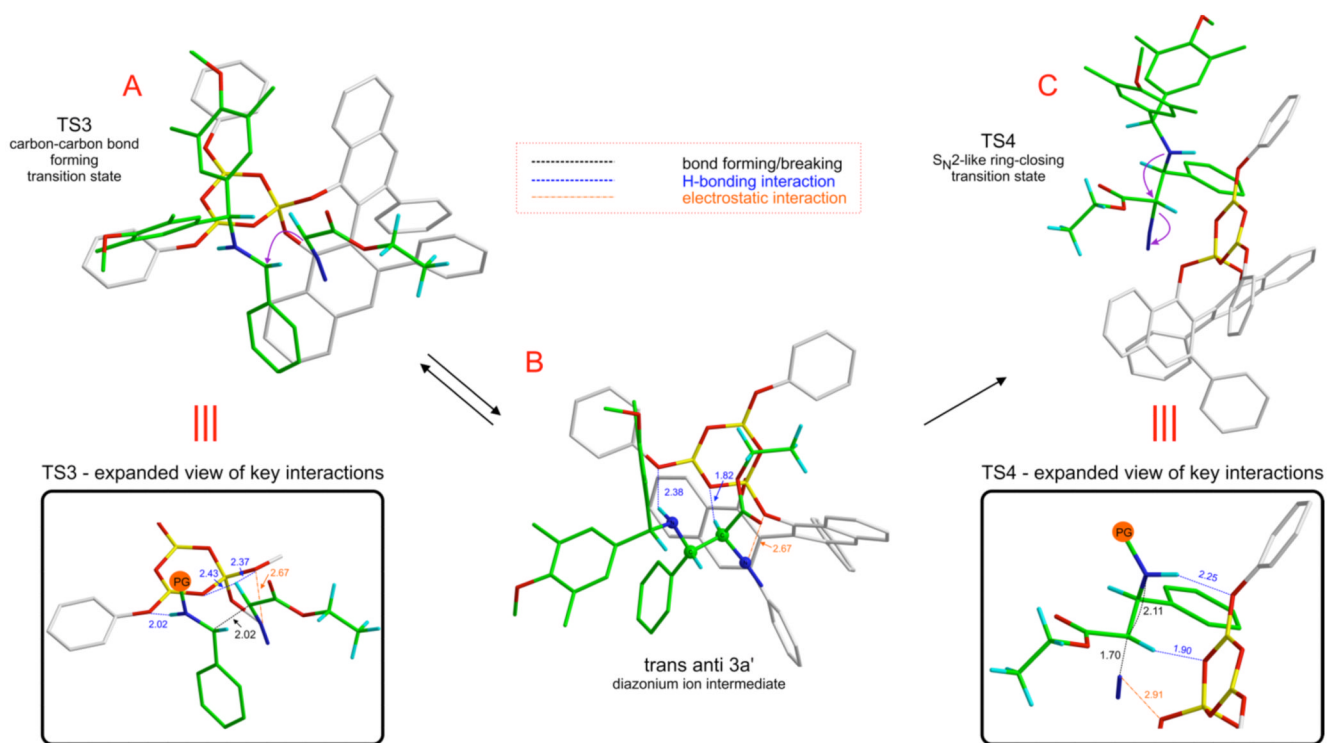


Figure 8.
Key stationary points on the reaction coordinate for the formation of *trans*-4a.

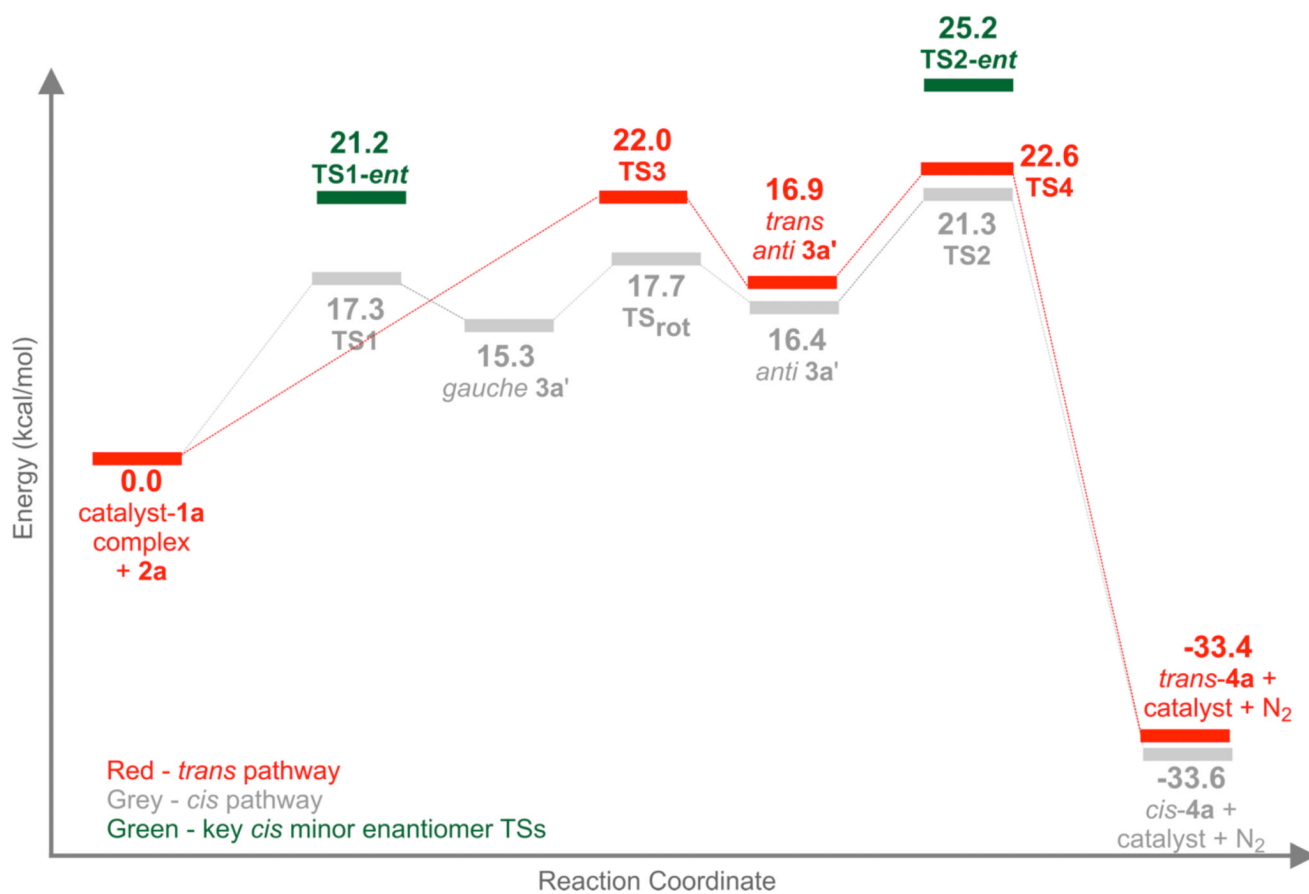
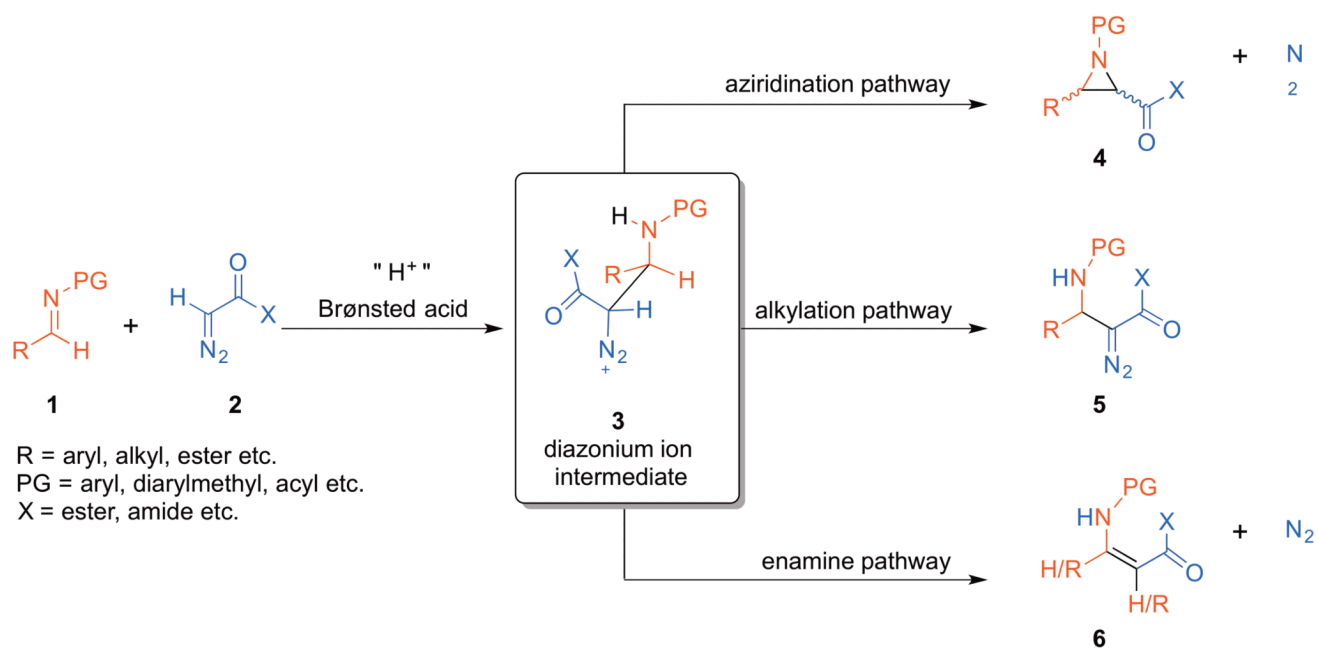
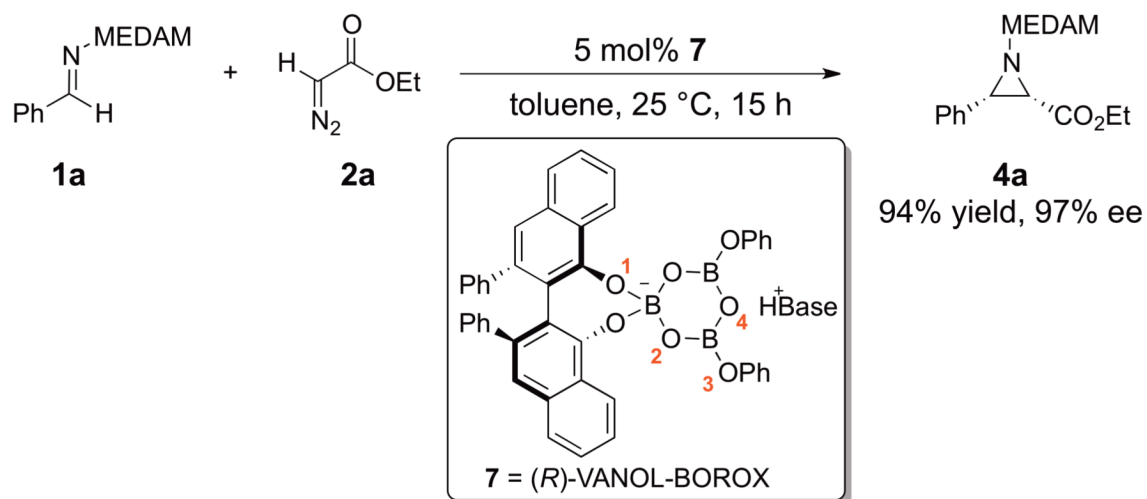


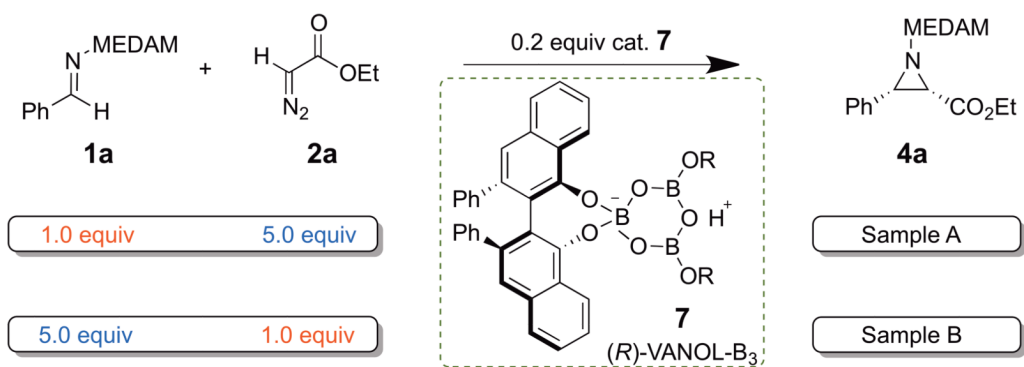
Figure 9. Overlay of the reaction coordinate Gibbs free energies (25 °C) for the *cis*- and *trans*-aziridination pathways along with key transition structures in the enantiomeric *cis* pathway.



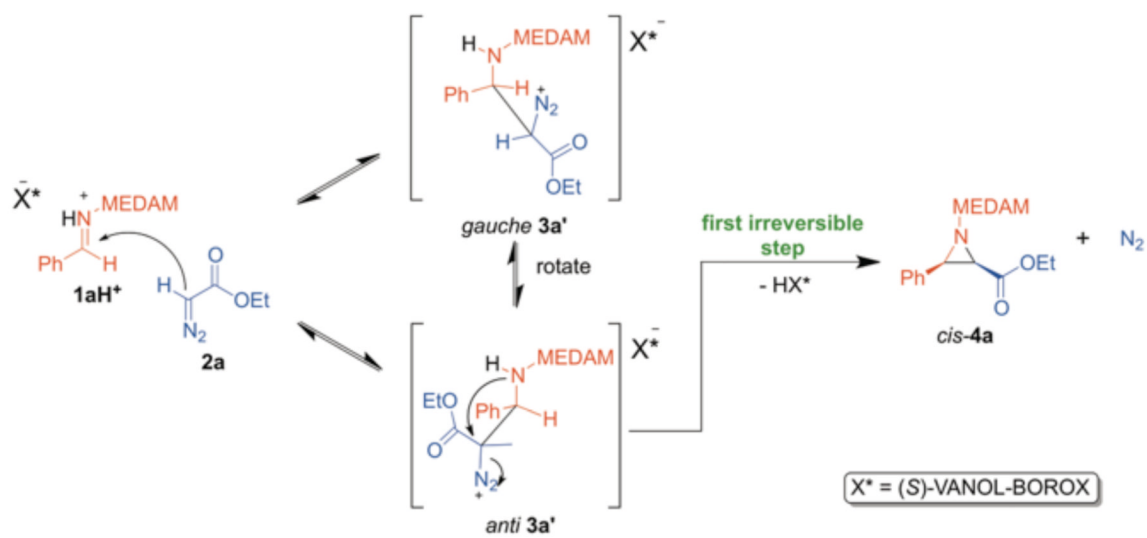
Scheme 1.
Diverging pathways of the putative diazonium ion intermediate 3

**Scheme 2.**

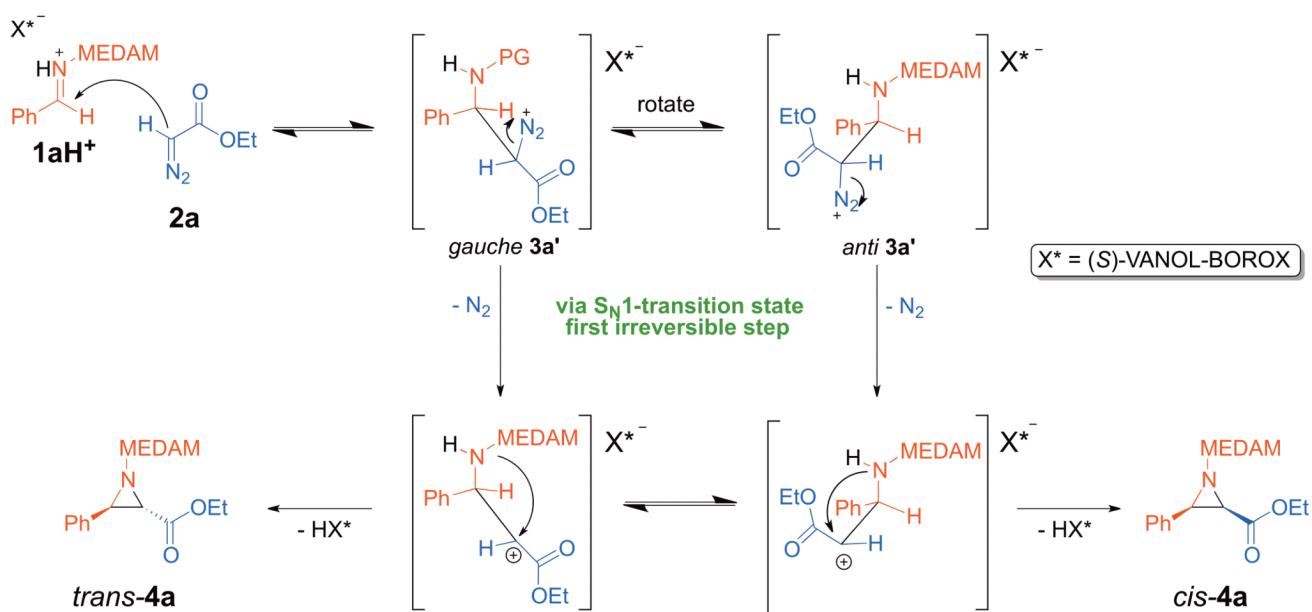
A typical aziridination reaction catalyzed by (*R*)-VANOL-BOROX catalyst



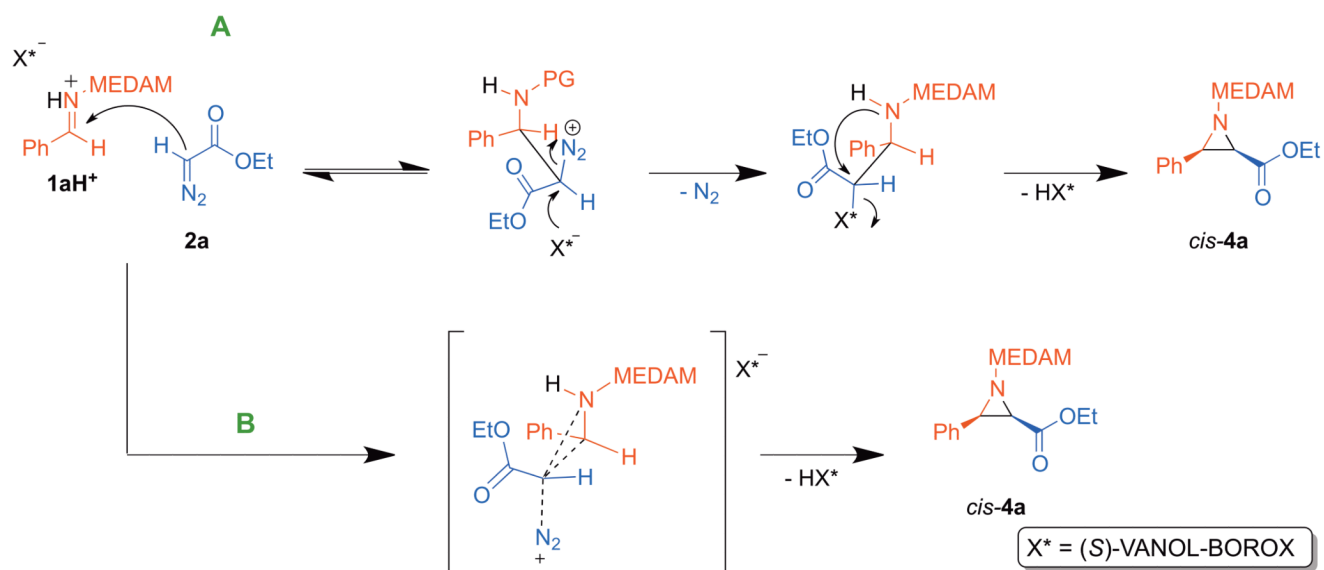
Scheme 3.
Design of experiment for the determination of intermolecular KIEs



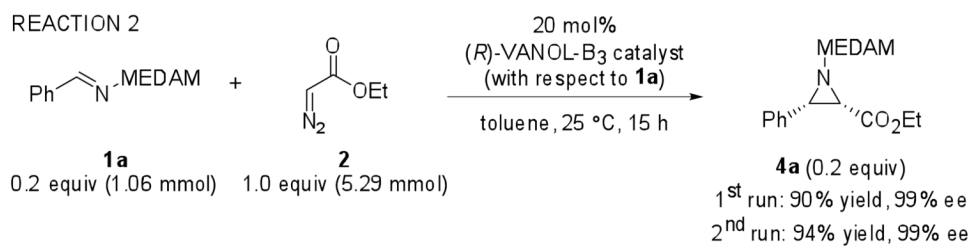
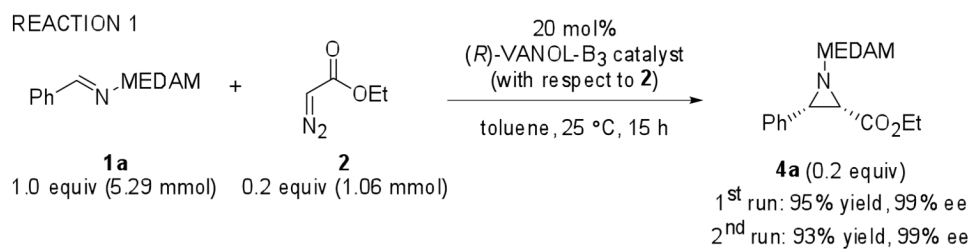
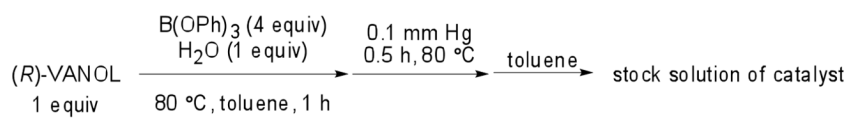
Scheme 4.
 $\text{S}_{\text{N}}2$ -like mechanism giving *cis-4a*



Scheme 5.
 S_N1 mechanism giving *cis-4a*



Scheme 6.
'Double displacement' and 'concerted' mechanisms leading to *cis-4a*.



Scheme 7.
Catalyst preparation and design of KIE experiments